

Article

Simultaneous Solution of Helical Coiled Once-Through Steam Generator with High-Speed Water Property Library

Yingjie Wu, Zhuo Jiang, Han Zhang *, Lixun Liu, Huanran Tang, Jiong Guo and Fu Li

Institute of Nuclear and New Energy Technology, Collaborative Innovation Center of Advanced Nuclear Energy Technology, Key Laboratory of Advanced Reactor Engineering and Safety of Ministry of Education, Tsinghua University, Beijing 100084, China

* Correspondence: han-zhang@tsinghua.edu.cn

Abstract: Efficient simulation of the helical coiled once-through steam generator (H-OTSG) is crucial in the design and safety analysis of the high-temperature gas-cooled reactor (HTGR). The physical property and phase transformation of water in the steam generator brings great challenges during simulation. The water properties calculation routine occupies a large part of the computational time in the steam generator solution process. Thus, a thermohydraulic property library is developed based on the IAPWS-IF97 formulation in this work to reduce the computational cost. Here the formulation adopts the backward equation method to avoid iterations in thermodynamic property calculation. Moreover, two Newton-method-based simultaneous solutions are implemented as implicitly nonlinear solvers, including Jacobian-Free Newton–Krylov (JFNK) and Newton–Krylov (NK) methods, due to its excellent computational performance. These simultaneous solution algorithms are combined with the developed water property library to simulate the H-OTSG efficiently. The numerical analysis is performed based on the transient and steady-state cases of the HTR-10 steam generator. Successful simulations of HTR-10 steam generator cases demonstrate the capability of the newly developed method.

Keywords: water property; IAPWS-IF97; H-OTSG; JFNK; NK



Citation: Wu, Y.; Jiang, Z.; Zhang, H.; Liu, L.; Tang, H.; Guo, J.; Li, F. Simultaneous Solution of Helical Coiled Once-Through Steam Generator with High-Speed Water Property Library. *Energies* **2023**, *16*, 1627. <https://doi.org/10.3390/en16041627>

Academic Editor: Michele La Rocca

Received: 16 December 2022

Revised: 27 January 2023

Accepted: 27 January 2023

Published: 6 February 2023



Copyright: © 2023 by the authors. Licensee MDPI, Basel, Switzerland. This article is an open access article distributed under the terms and conditions of the Creative Commons Attribution (CC BY) license (<https://creativecommons.org/licenses/by/4.0/>).

1. Introduction

Featuring the compact structure, high heat transfer efficiency, and the ability in high thermal expansion, helical coiled once-through steam generators (H-OTSG) have been widely used in the new type of nuclear power plants. Therefore, H-OTSG is equipped in high-temperature gas-cooled reactors (HTGRs), aiming to realize modular construction and competitive economic benefits. In the H-OTSG, the primary side coolant generally flows from top to bottom outside helical tubes (shell side), while the secondary side water flows from bottom to top inside the tubes (tube side). The helical structure is similar to a spring, which can withstand the stress caused by thermal expansion and improve the reliability of the steam generator. Complex flow and heat exchange characteristics make H-OTSG one of the most important pieces of equipment for an HTGR. Meanwhile, the H-OTSG's working condition is very critical. Since the working temperature is 750 °C, or even higher, thermal analysis of H-OTSG becomes very important.

The steam generator simulation should be considered carefully in the reactor safety analysis procedure. Especially in HTGR systems, studies on steady state and transients in H-OTSG are essential in analyzing overall reactor performance as well as designing the appropriate control systems [1]. Due to their compact structure and wide range of applications, research on H-OTSG simulation programs has gradually increased. Most studies focus on flow heat and transfer in the helical tube with high-temperature water [2–5]. Some scholars carried out experiments of helical tubes under large ranges of operating conditions to acquire detailed heat transfer characteristics [6,7]. Little research has been

carried out on efficiency analysis of steam generator codes. Through detailed investigation and analysis, this study focuses on factors that affect efficiency and optimization methods.

The use of water and steam in an H-OTSG makes the evaluation of its thermodynamic properties a critical issue. According to the existing research on the steam generator and our previous research, property evaluation time dominated the whole calculation time [8]. The two-phase state created the demand for reliable approaches for the fast evaluation of thermodynamic properties. The commonly used formulations for calculating water and steam properties contain scientific and industrial standards. The International Association for the Properties of Water and Steam, IAPWS, developed the formulation IAPWS-95 for accurate scientific property calculation [9]. The formulations cover a wide range of conditions and are consistent from the thermodynamic point of view and accurate for experimental data. Most scientific standards are based on the fundamental equation, the Helmholtz and Gibbs free energy. The details can be referred to in Keenan's work [10]. However, such formulations are orientated to the production of property tables rather than to meet the need of engineering computations. Formulations for fast calculation have also been extensively studied. Sail and Wanger developed the formulations for fast simulation propose [11]. The formulations have a 38-coefficient expansion and can provide a sufficient range in industrial calculations. Fernandes' work presents the cubic equations to estimate the thermodynamic properties of superheated steam [12]. The results show that the equations are adequate within the range of operation for most of the steam power plant. The IAPWS also proposed a set of formulations for industry application in 1997, which is called IAPWS-IF97 [13]. It is widely used in industrial applications due to its high computing efficiency and wide range of validity. In general, the demand for fast calculation of the thermodynamic properties of water and steam is increasing in industrial applications, and the same need exists for steam generator simulation. For the selection of the formulations of thermodynamic properties, more attention was paid to the accuracy, efficiency, and range of validity. According to the research on the thermodynamic property formulation and the requirements of the steam generator, a water and steam property library for the H-OTSG was developed based on the IAPWS-97 formulation.

To efficiently solve the steam generator, attention should be paid to the fast convergence rate and high-stability algorithms as well. There are different fluids on the primary and secondary sides of the H-OTSG. The most direct way is to solve the two flow areas separately and converge iteratively, which is also the treatment in traditional steam generator code. The convergence will be slow in a fast-responding system such as H-OTSG, and the same situations will occur in many calculations. Simultaneous solution methods such as Newton's methods have drawn much attention in nuclear engineering analysis code [14–17] and achieved good results in steam generator simulation [8,18]. Newton–Krylov (NK) and Jacobian-free Newton–Krylov (JFNK) methods are two variants for solving nonlinear systems [19–21]. The advantage of the Newton–Krylov method is its stability, while the JFNK method pays more attention to improving computational efficiency. The principles of the two methods can be found in the literature [22], and our previous work also applied them to the steam generator model [8,18]. The numerical simulation of thermal–hydraulic processes in H-OTSG requires very accurate and high-speed algorithms for calculating water and steam thermophysical properties. Combined with our developed water property library, the overall calculation efficiency can be greatly improved. Due to the implementation of the backward equation method in the library [23], some truncation errors will be introduced during the calculation process. A comprehensive analysis of the accuracy and efficiency between the backward equation method and the original method is discussed in this work. The results illustrate that this backward method can greatly improve the efficiency while guaranteeing the accuracy.

The movable boundary steam generator numerical model is applied to test the above improvements. This steam generator numerical model can provide reliable results and significantly reduce computing costs. In combination with the movable boundary model, Newton's algorithms, and the efficient water properties formulation, an efficient method

for solving H-OTSG problems is developed and thoroughly investigated in this work. All the progress is integrated into the H-OTSG simulation code. The analysis of HTR-10 H-OTSG steady-state conditions is carried out in this paper, which verifies the efficiency and accuracy of our fast calculation method. Meanwhile, the transient conditions of HTR-10 H-OTSG are also analyzed to prove the dynamic simulation ability of the code.

2. Thermodynamic Properties in H-OTSG Simulation

Industrial demands for calculating water and steam properties have long received extensive attention. The first industrial formulation for the thermodynamic properties of water and steam was proposed in 1960 [24], which satisfies the need for accuracy and efficiency. The updated formulation was proposed in 1997 and abbreviated to IAPWS-IF97. The developments of these formulations illustrate the need for the industry to calculate water and steam properties, with particular attention to the efficiency and accuracy of the formulations. Especially for H-OTSG in HTR power cycles, thermodynamic properties of subcooled water to super-heated steam need to be calculated repeatedly. Regarding the three criterions' accuracy, consistency along region boundaries, and computation speed, IAPWS-IF97 is adequate during H-OTSG simulation. Hence, a library based on IAPWS-IF97 is developed for thermodynamic property evaluation in H-OTSG's calculation.

2.1. Basic Theory for IAPWS-IF97

The range of validity in IAPWS-IF97 formulation is defined by the following temperature and pressure:

$$0\text{ }^{\circ}\text{C} \leq t \leq 800\text{ }^{\circ}\text{C} \quad p \leq 100\text{ MPa}$$

For high-temperature applications, such as in gas turbines, the following extension of the range of validity was requested:

$$800\text{ }^{\circ}\text{C} < t \leq 2000\text{ }^{\circ}\text{C} \quad p \leq 10\text{ MPa}$$

While for H-OTSG operating conditions in HTR, the temperature and pressure range of water or steam is within

$$100\text{ }^{\circ}\text{C} \leq t \leq 600\text{ }^{\circ}\text{C} \quad 5 \leq p \leq 30\text{ MPa}$$

This indicates that IAPWS-IF97 meets the calculation requirements of thermodynamic properties in H-OTSG. As shown in Figure 1, the entire range of validity was divided into five regions with different equations. Region 1 and region 2 are covered by the basic equations of the specific Gibbs free energy $g(p, T)$, while region 3 is covered by the basic equation of the specific Helmholtz free energy $f(\rho, T)$. Region 4 is the saturation–pressure equation $P_s(T)$ of the two-phase region (corresponding to the saturation curve in the p – T diagram). High-temperature region 5 is also covered by equation $g(p, T)$. These five equations are the so-called basic equations. The Helmholtz and Gibbs free energies describe the behavior of a particular system, and the difference between them is that Gibbs free energy is defined under constant pressure while Helmholtz free energy is defined under constant volume [25].

Based on the basic equations for the H-OTSG most important regions (1, 2, and 4), the following thermodynamic properties could be directly calculated with a function of p and T : specific volume v , specific enthalpy h , specific entropy s , specific isobaric heat capacity c_p , and the saturation pressure p_s as a function of T . If there is a need to calculate other combinations of variables, for example, the combinations $v(p, h)$, $T(p, h)$, $s(p, h)$, $h(p, s)$, $T(p, s)$, and $T_s(p)$, these had to be determined via corresponding iterations. Due to these iterations in combination with a relatively complex structure of the equations, calculations for the H-OTSG with the old industrial standards IFC-67 and scientific standard IAPWS-95 required relatively long computing times.

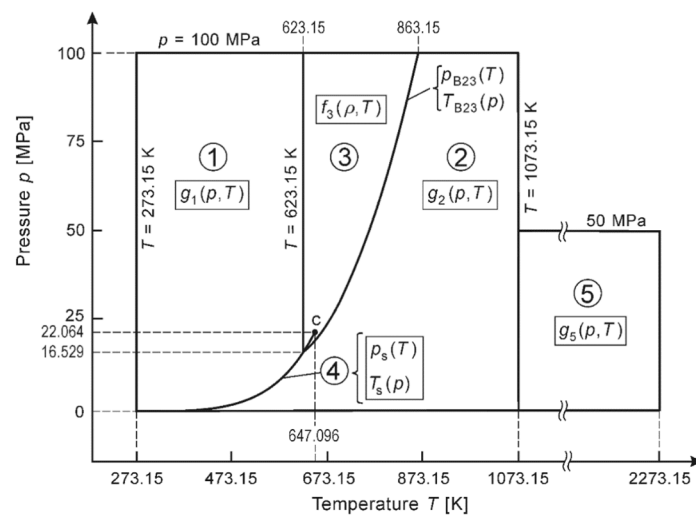


Figure 1. Regions and equations of IAPWS-IF97 [26].

However, IAPWS-IF97 equations were developed to meet the main requirement of a short computing time. The structure of the equations was optimized which allowed short computing times and maintaining accuracy and consistency along region boundaries [27]. In addition, all those thermodynamic properties which are not direct functions of the independent variables of the basic equations are not found by iteration from the basic equations. Instead of this, so-called backward equations were developed, namely, equations $T(p, h)$ and $T(p, s)$ for regions 1 and 2 and $T_s(p)$ for the saturation curve. All the combination functions can be calculated without any iteration under these backward equations.

2.2. Development and Application of Water Library in H-OTSG

Computation speed is the most essential demand for thermodynamic properties' evaluation. For H-OTSG simulation, the main requirement regarding the computation speed was calculating all property functions listed in Table 1. The frequency of properties is based on the survey of thermodynamic property calculation among the power industries, which is similar to steam generator simulation. During the operation of the steam generator, the state of water and steam is in regions 1, 2, and 4. In addition, Table 1 also gives the average frequencies of the most important property functions in these regions.

As mentioned in the previous subsection, the backward equations could improve computing efficiency. In the actual simulation process, some variables will be calculated by backward equations while others will be calculated by basic equations. However, the simulation required that the numerical consistency between the backward and the basic equations was extremely good. Otherwise, it would have caused numerical problems when "jumping" back and forth between the basic and the backward equations, for example, when calculating the steady state in the steam generator. Although the permissible numerical inconsistencies between the basic and backward equations are relatively small, these inconsistencies may affect the two phases boundary in helical tubes. Especially when the state of each position in the steam generator is solved by the simultaneous coupling method, whether the inconsistency will lead to the numerical divergence still needs further exploration. The discussion on this aspect will be described in Section 4. At the same time, we will also give a comparison of accuracy and efficiency under industry standards and scientific standards in H-OTSG simulation.

Table 1. Most important property functions and their frequency of use [23].

Region	Function	Frequency of Use %
1 (Liquid)	$v(p, T)$	2.9
	$h(p, T)$	9.7
	$T(p, h)$	3.5
	$h(p, s)$	1.2
		4.7
2 (Vapor)	$v(p, T)$	6.1
	$h(p, T)$	12.1
	$s(p, T)$	1.4
	$T(p, h)$	8.5
	$v(p, h)$	3.1
	$s(p, h)$	1.7
	$T(p, s)$	1.7
	$h(p, s)$	4.9
		13.3
4 (Saturation)	$p_s(T)$	8.0
	$T_s(p)$	30.7
	$h'(p)$	2.25
	$h''(p)$	2.25
		6.6
		35.2
Sum		100.0
		59.8

In this study, a water library is developed according to IAPWS-IF97 formulation and the main equations are presented in this part. The main purpose of these equations is to calculate water and steam properties, and the margin of each relation is listed. As mentioned in the previous subsection, the basic equation and backward equation of each region will be discussed for different properties calculations. The forms of these equations are given and the corresponding references are given, respectively. The equations [26] in region 1 are listed in Table 2.

Table 2. Relations for region 1 in IAPWS-IF97.

Basic Equation	Backward Equation
$g_1(p, T) = RT \cdot \gamma(p, T)$ $273.15 \text{ K} \leq T \leq 623.15 \text{ K}$ $p_s(T) \leq p \leq 100 \text{ MPa}$	$T_1 = \theta(p, h)$ $273.15 \text{ K} \leq T \leq 623.15 \text{ K}$ $p_s(T) \leq p \leq 100 \text{ MPa}$ except for the meta stable region

Region 2 basic equation [26] $f(p, T)$ and backward equation [26] $T(p, h)$ are listed in Table 3, while in metastable region, region 2 modified basic equation [26].

Table 3. Relations for region 2 in IAPWS-IF97.

Basic Equation	Backward Equation
$g_2(p, T) = RT \cdot \gamma(p, T)$ $g_2'(p, T) = RT \cdot \gamma(p, T)$ (meta stable region) $273.15 \text{ K} \leq T \leq 623.15 \text{ K}$ $0 < p \leq p_s(T)$ $623.15 \text{ K} < T \leq 863.15 \text{ K}$ $0 < p \leq p(T)$ $863.15 \text{ K} < T \leq 1073.15 \text{ K}$ $0 < p \leq 100 \text{ MPa}$	$\left\{ \begin{array}{l} T_{2a} = \theta(p, h) \\ T_{2b} = \theta(p, h) \\ T_{2c} = \theta(p, h) \end{array} \right.$

Region 2 basic equation saturation pressure [26] $p_s(T)$ and backward equation [26] saturation temperature $T_s(p)$ are shown in Table 4

Table 4. Relations for saturation regions in IAPWS-IF97.

Basic Equation	Backward Equation
$p_s = p_s(T)$ $273.15 \text{ K} \leq T \leq 647.096 \text{ K}$	$T_s = T_s(p)$ $611.213 \text{ Pa} \leq p \leq 22.064 \text{ MPa}$

Dynamic viscosity equation [28]:

$$\eta = \eta(\rho, T)$$

Equation of surface tension [26]:

$$I = I(T)$$

$$273.15 \text{ K} \leq T \leq 647.096 \text{ K}$$

Equation of thermal conductivity [29]:

$$\lambda = \lambda(\rho, T)$$

In fact, the dynamic viscosity and thermal conductivity are first solved by pressure and temperature, and then the corresponding function is called by density and temperature.

The equations can be referred to in the literature [26]. It should be noted that the method for calculating heat capacity and density using enthalpy and pressure is not given in the formulation. We solve this problem by combining the basic equations with the backward equations. The key to the properties' calculation is to use different equations depending on the input variables.

3. Model and Numerical Methods

Another improvement of this work is the efficient numerical methods. In this section, the advanced numerical methods and the steam generator model used in this work are briefly discussed. All these techniques will be devoted to this work to solve the steam generator model efficiently.

3.1. Overview of H-OTSG Model and Newton's Methods

The helical coiled once-through steam generator (H-OTSG) is often used in modular reactors and is slightly different from other steam generators. Based on the movable boundary steam generator model [30], the heat exchange pipes inside the steam generator are divided into three parts: subcooled region, nucleate boiling (two-phase) region, and superheated region. The thermal–hydraulic dynamic behaviors in these regions are described using the basic conservation equations, and the alterable control volumes are used to capture the different heat exchange and flow characteristics. Movable boundary models have been added to our previous work, and the equations can refer to Zhu's work [31]. The physical properties used in the dynamic model are mainly referred to the steam generator reports. The heat transfer correlations are selected in the HTR-10 steam generator thermal–hydraulic design [32]. The friction model for the two-phase water in helical coiled tube is calculated by Xian University's correlation equations [33]. These correlations agree well with experimental data and simulations.

The movable boundary method could significantly reduce the number of unknowns. Nevertheless, solving this system will also need many iterations due to the different thermohydraulic characteristics of the primary and secondary sides. Newton's method with simultaneous coupling characteristics will be applied to increase the convergence rate. In addition, two variants of this method, Newton–Krylov and Jacobian-free Newton–Krylov (JFNK), are used to solve the nonlinear system. The advantages and characteristics of both methods were discussed in our previous work, and here we focus more on their validity to new problems. In the movable boundary method, the number of solution variables will be reduced by magnitude compared to the finite volume method. In this case, the

cost of Jacobian matrix calculation in the Newton–Krylov method will be significantly reduced. Tight coupling of the system due to highly simplified model will result in an increase in Jacobian-free process error in the JFNK method. This might result in a slower convergence rate during iterations. In this situation, the cost of constructing the Jacobian in the Newton–Krylov method and the convergence rate in the JFNK method needed to be re-evaluated. For this kind of nonlinear system, the efficiency and precision of the two methods needed to be analyzed in detail. Owing to the scientific computational toolkit PETSc package [34], the Newton–Krylov and JFNK methods are implemented in our work. It should be noted that the preconditioner is the key to improving the efficiency and stability of the JFNK method. Some original work on preconditioners has been studied in our previous work, and here we follow the previous approach.

3.2. Fast Simulation Method for H-OTSG

The above subsections discuss the special treatments for fast simulation in the H-OTSG problem. Another attempt for the fully implicit discretization of the governing equations is performed based on the first-order backward Euler method. Due to the implementation of the JFNK method and Newton–Krylov method, a nested iterative method is proposed, consisting of four levels. The flow chart of the method is shown in Figure 2. The primary level is the loop over the Newton correction and the loop building up the Krylov subspace by GMRES approach, out of which Newton correction is drawn. However, the JFNK method and Newton–Krylov method differ in the calculation of matrix-vector products in the GMRES iterations. Outside the Newton loop, a line-search technique is used for global convergence, and a physical preconditioner is applied interior to the Krylov loop. In the innermost iteration, all physical properties need to be updated first, which requires the water properties formulations. Then, according to the movable boundary model, the residual functions for the Krylov subspace are established.

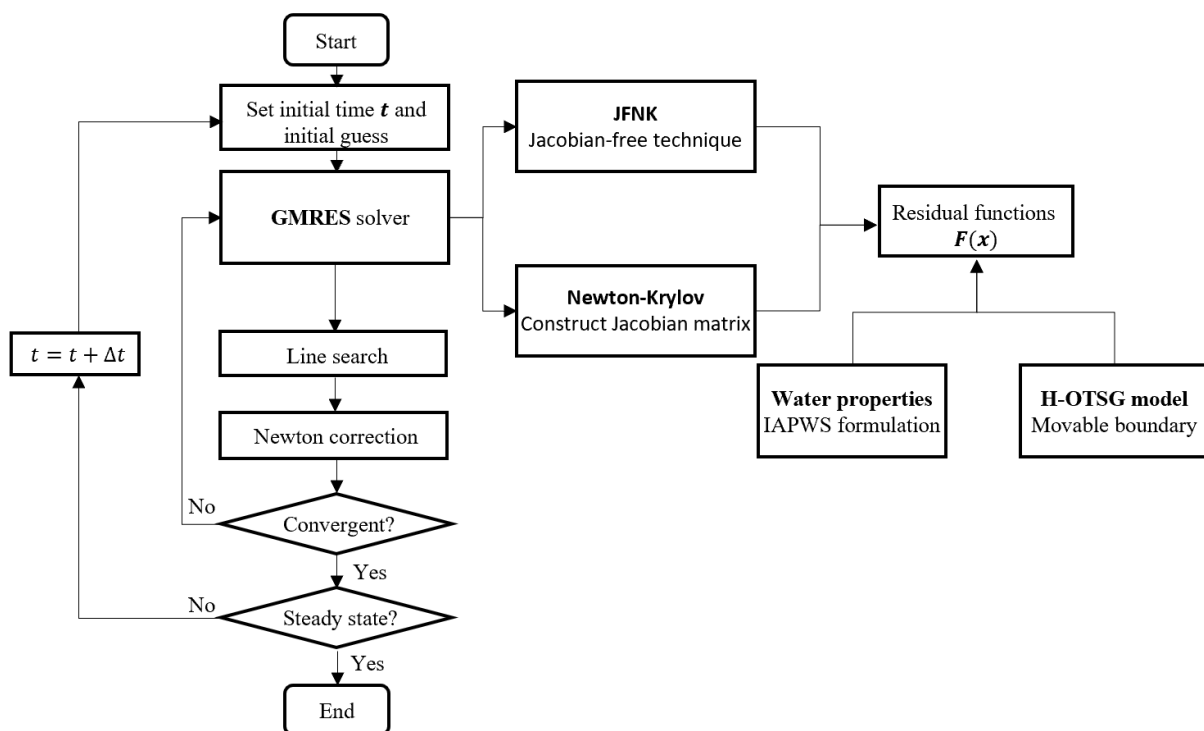


Figure 2. Flow chart of the fast simulation method for H-OTSG.

Excessive calculation cost and high-precision requirements are two major problems in H-OTSG simulation. In this developed methodology, the JFNK method will be used to improve the convergence rate, and high-speed water property library will be used to reduce

the water properties calculation time. However, the two methods might have problems in convergence robustness and accuracy. Detailed analysis will be given in the next section, including the reliability of the developed water library and the efficiency comparison of different algorithms.

4. Result and Discussion

As described in Sections 2 and 3, the developed method pursues efficient and accurate simulation of H-OTSG, main contributions include the Newton's algorithms and high-speed water properties formulation. Although the IAPWS-IF97 formulation is reliable, verifying and analyzing the deviation between the property library we developed and the accurate scientific formulation is still necessary. The high-precision properties computing library CoolProp is employed in this work, which provides IAPWS-95 formulation as a comparison [35]. A steam generator simulation code using movable boundary model is developed based on the high-performance numerical library PETSc [34]. A comparative analysis of the models was completed in our previous work [18]; here, we focus more on the performance of the new methods. This section will be divided into two parts. The first part verifies the accuracy of the self-developed property library. In the second part, numerical and fast calculation methods of thermodynamic properties are applied to solve the steam generator model, and the accuracy and efficiency of various methods are also analyzed. The work allows the calculation of the transient and steady-state HTR-10 steam generator model to demonstrate the accuracy and efficiency of the code. Due to the strong dependency on the initial guess, the analysis of the convergence characteristics is carried out in a steady-state condition. The transient analysis is relatively preliminary. At present, only the core parameter, steam generator outlet temperature, is compared under three transient conditions, and reliability analysis is given.

4.1. Comparison of Thermodynamic Properties

In this subsection, the water properties calculated by IAPWS-95 scientific standard are taken as the benchmark because the formulation uses the basic equation and strict iterative algorithm. The results of the developed library based on IAPWS-IF97 will be compared with the benchmark solution. The key parameters need to be validated, such as enthalpy h , specific heat capacity C_p , density ρ , and surface tension I , which are used in steam generators for damping coefficient. However, the dynamic viscosity ν and thermal conductivity λ are calculated by the backward equation $f(\rho, T)$ in the IAPWS-IF97 formulation, where the density ρ needs to be solved by basic function $g(p, T)$. The results of the calculation and comparison are shown in Table 5 and Figure 3. The range of pressure is 0.0035~20 MPa, and the temperature range is from 300 K to 600 K.

As shown in Table 2, compared with IAPWS-95, the smallest relative error is not surface tension but dynamic viscosity, and the maximum is the thermal conductivity, which is 3.23%. Moreover, the average relative error of specific heat capacity C_p and saturation pressure is about 0.01% and the average relative error of enthalpy and entropy is 0.001%. In addition, with the increase of pressure, the relative error of thermal conductivity λ has an increasing trend, but other variables remain basically unchanged. In general, the relative errors are all within 0.5%, excepting the thermal conductivity λ and the saturation temperature T_s . The maximum relative error of saturation temperature is within 2%. It should be noted that the location of the maximum relative error is often random, but the error increases at the edge of the computation region. As an example of saturated temperature T_s , as shown in Figure 4, the relative error is greater at 20 MPa because it is near the edge of region 4.

Table 5. (a) The relative error in $f(p,T)$ compared with IAPWS-95. (b) The relative error in $f(p,T)$ compared with IAPWS-95.

(a)							
	p/Mpa	T/K	$h/\%$	$s/\%$	$C_p/\%$	$\rho/\%$	$v/\%$
Case1	0.0035	300	1.14×10^{-3}	4.85×10^{-4}	2.20×10^{-1}	9.88×10^{-4}	9.63×10^{-6}
Case2	0.0035	500	3.69×10^{-4}	3.46×10^{-4}	7.61×10^{-3}	1.72×10^{-3}	1.80×10^{-4}
Case3	0.0035	600	1.98×10^{-4}	3.11×10^{-4}	3.53×10^{-3}	1.41×10^{-3}	2.01×10^{-4}
Case4	1	450	1.75×10^{-2}	1.35×10^{-2}	2.16×10^{-2}	6.15×10^{-4}	1.69×10^{-3}
Case5	1	440	1.66×10^{-2}	1.25×10^{-2}	4.57×10^{-2}	3.13×10^{-4}	8.68×10^{-4}
Case6	1.5	450	1.77×10^{-2}	1.39×10^{-2}	2.15×10^{-2}	6.35×10^{-4}	1.15×10^{-3}
Case7	3	300	8.91×10^{-3}	9.12×10^{-3}	1.16×10^{-2}	1.06×10^{-4}	2.23×10^{-5}
Case8	3	500	3.51×10^{-3}	3.45×10^{-3}	9.54×10^{-2}	6.66×10^{-4}	1.14×10^{-3}
Case9	10	600	4.73×10^{-3}	4.57×10^{-3}	8.22×10^{-2}	8.03×10^{-3}	8.20×10^{-5}
Case10	20	300	8.24×10^{-3}	9.61×10^{-3}	1.62×10^{-2}	1.11×10^{-3}	3.32×10^{-5}

(b)						
	p/Mpa	T/K	$\lambda/\%$	$l/\%$	$P_s/\%$	$T_s/\%$
Case1	0.0035	300	6.78×10^{-5}	1.16×10^{-1}	6.24×10^{-3}	3.98×10^{-4}
Case2	0.0035	500	1.36×10^{-6}	6.59×10^{-1}	1.15×10^{-2}	3.98×10^{-4}
Case3	0.0035	600	2.45×10^{-5}	8.99×10^{-1}	3.93×10^{-3}	3.98×10^{-4}
Case4	1	450	1.17×10^{-1}	3.44×10^{-1}	1.75×10^{-2}	1.68×10^{-3}
Case5	1	440	7.42×10^{-2}	2.86×10^{-1}	1.65×10^{-2}	1.68×10^{-3}
Case6	1.5	450	1.16×10^{-1}	3.44×10^{-1}	1.75×10^{-2}	1.75×10^{-3}
Case7	3	300	3.44×10^{-4}	1.16×10^{-1}	6.24×10^{-3}	1.07×10^{-3}
Case8	3	500	3.58×10^{-1}	6.59×10^{-1}	1.15×10^{-2}	1.07×10^{-3}
Case9	10	600	3.23×10^0	8.99×10^{-1}	3.93×10^{-3}	4.26×10^{-4}
Case10	20	300	1.57×10^{-3}	1.16×10^{-1}	6.24×10^{-3}	1.68×10^0

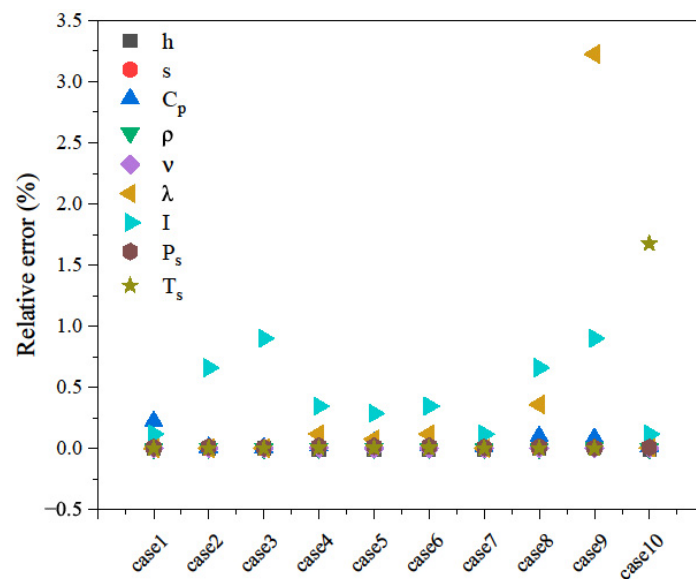


Figure 3. Relative error in $f(p, T)$.

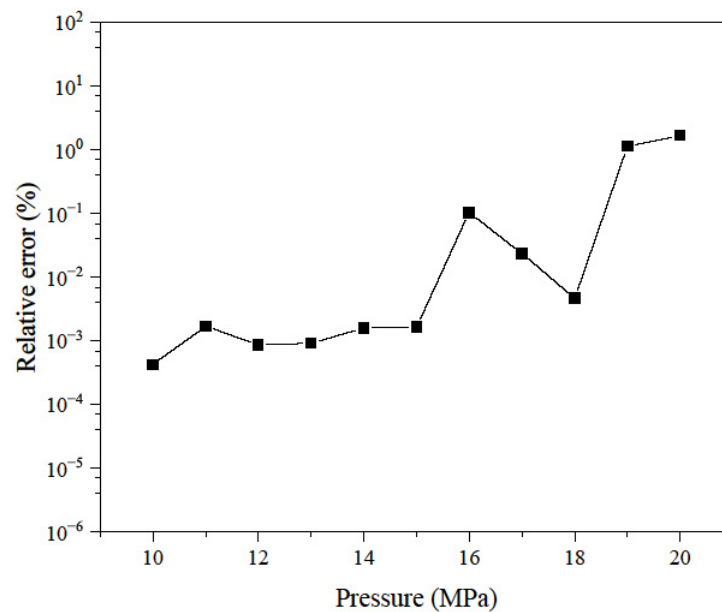


Figure 4. Relative error in T_s with different pressure.

During H-OTSG simulation, thermodynamic properties need to be determined by enthalpy and pressure when temperature cannot be obtained. This situation also exists in the algorithm implementation process, because sometimes temperatures are treated as the intermediate variables to compute enthalpy. The relative errors of the backward equation $f(p, h)$ are listed compared with IAPWS-95 formulation. The calculated results are shown in Table 6 and Figure 5. It can be seen from the calculation results that the maximum relative errors of the three parameters are all within 1%. The maximum relative deviation is 0.806% in density.

Table 6. The relative error in $f(p, h)$ compared with IAPWS-95.

	p/Mpa	$h \text{ KJ/kg}$	$T/\%$	$Cp/\%$	$\rho/\%$
Case1	0.001	3000	8.08×10^{-1}	1.26×10^{-1}	8.00×10^{-1}
Case2	3	500	3.45×10^{-3}	6.60×10^{-2}	1.39×10^{-3}
Case3	3	3000	8.84×10^{-2}	5.32×10^{-2}	1.17×10^{-1}
Case4	3	4000	4.65×10^{-3}	7.88×10^{-3}	7.80×10^{-3}
Case5	5	3500	9.64×10^{-3}	6.14×10^{-2}	1.09×10^{-2}
Case6	5	4000	7.31×10^{-3}	5.12×10^{-3}	-1.29×10^{-2}
Case7	25	3500	1.38×10^{-3}	8.74×10^{-2}	1.19×10^{-3}
Case8	40	2700	4.59×10^{-4}	1.21×10^{-1}	2.68×10^{-2}
Case9	60	2700	1.27×10^{-3}	3.95×10^{-1}	1.87×10^{-2}
Case10	60	3200	4.21×10^{-3}	1.00×10^{-1}	2.92×10^{-3}

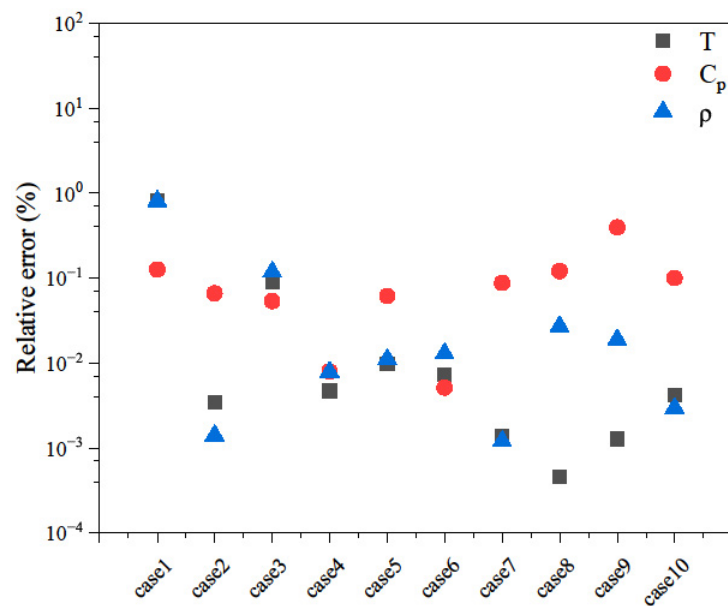


Figure 5. Relative error in $f(p, h)$.

In summary, except for thermal conductivity, saturation temperature, and surface tension, the relative error of other parameters is about 0.01%. The water property evaluations are acceptable and prove that the property library developed is reliable. Thermodynamic properties with large errors are often used in calculating heat exchange coefficient. In particular, the saturation temperature is used to calculate the position of the gas–liquid interface. Therefore, the effect of these deviations on the actual calculation needs to be evaluated in the H-OTSG simulation.

4.2. Steady-State H-OTSG Model in HTR-10

Table 7 shows the simulation results of the HTR-10 full-condition H-OTSG model, and the key parameters concerned with in steam generator design can be found in reference [18]. It is worth noting that the abbreviation “IF97” refers to our developed property library, and “95” refers to the scientific formulation used in the CoolProp library. From these results, it is evident that both algorithms and water properties routines can obtain precise simulation results. The current results can meet engineering design requirements, and a detailed illustration can be found in the reference [7]. In this case, the outlet water temperature obtained with the assistance of the IAPWS-IF97 formulation is 0.5 °C lower than the original routine, proving the consistency of the developed library and the scientific standard. It should be emphasized that although the movable boundary model is not the most accurate steam generator model, it can still provide accurate outlet parameter results for steam generator design. Table 8 shows the computation time with different algorithms and water properties evaluation routines. Due to the explicit construction of the Jacobian matrix through finite difference, the Newton–Krylov method spends more time in Jacobian matrix evaluation. Therefore, the Newton–Krylov method requires more than twice the computation time of the preconditioned JFNK method in steam generator simulations. The main computational cost of the JFNK method lies in the evaluation of residual function, mainly because of the approximated matrix-vector product used in Krylov iterations. Both algorithms require the same nonlinear iterations, but the low calculation cost in the JFNK method accelerates the overall solution. It can be found in Table 8 that the water properties calculation routine using the IAPWS-IF97 formulation will significantly reduce the calculation time. This efficient method uses approximated equations and avoids iteration in calculating water properties. Despite the loss of calculation accuracy, the code using backward equations will reduce the calculation time to 30% of the original method.

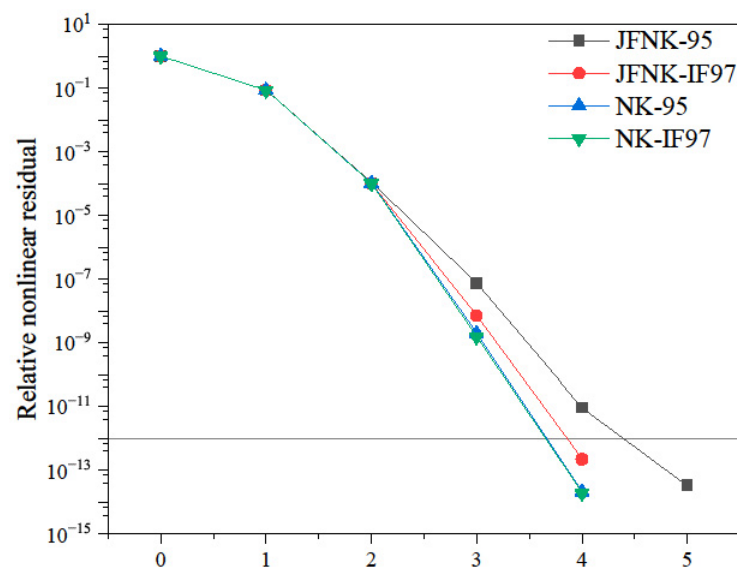
Table 7. Simulation results in steady-state HTR-10 steam generator model using different algorithms and water properties routines.

	JFNK-95	JFNK-IF97	NK-95	NK-IF97	Ref
Length of subcooled region (m)	14.65	14.63	14.65	14.63	14
Length of nucleate boiling region (m)	14.56	14.56	14.56	14.56	14
Temperature of outlet water(m)	466.50	466.12	466.50	466.12	465
Pressure of outlet water (Pa)	4272.99	4270.43	4272.99	4270.43	4300

Table 8. Numerical computation time occupied by each part in the simulation.

	JFNK-95	JFNK-IF97	NK-95	NK-IF97
Total computation time (ms)	2380.82	786.55	9293.08	3275.88
Evaluation time of residual function (ms)	898.98	332.02	186.96	140.15
Numbers of residuals function evaluations	44	35	5	5
Evaluation time of preconditioner/Jacobian matrix (s)	143.01	84.12	9048.30	3083.60
Numbers of preconditioner/Jacobian matrix evaluations	4	4	4	4

The nonlinear residual history during steady-state simulation is demonstrated in Figure 6. The reference line in the graph represents the relative nonlinear convergence criteria $rtol = 10^{-12}$ selected in this work. As shown, all four methods have good nonlinear convergence rates. The Newton–Krylov method with the precise Jacobian matrix has a faster convergence rate, while the two different water properties formulations do not affect the convergence rate. Since the JFNK method demands on a large numbers of residual function evaluations, the convergence characteristic will be easily affected by the different water properties formulations within the residual functions. Fortunately, this deviation is slight and does not change the overall nonlinear convergence characteristics.

**Figure 6.** Nonlinear residual history in steady-state HTR-10 steam generator simulation.

In order to further investigate the performance of the backward equation method, comparisons between two water properties formulations are made in the steady case. Since the residual evaluations are needed in the linear iteration process of the JFNK method, the water properties formulations might affect the linear solution. Linear residual history

in the JFNK method has been summarized, as shown in Figure 7. The calculation error caused by the backward equations has no significant influence on the linear convergence rate, which means that the two methods are very effective for HTR-10 steam generator operation condition.

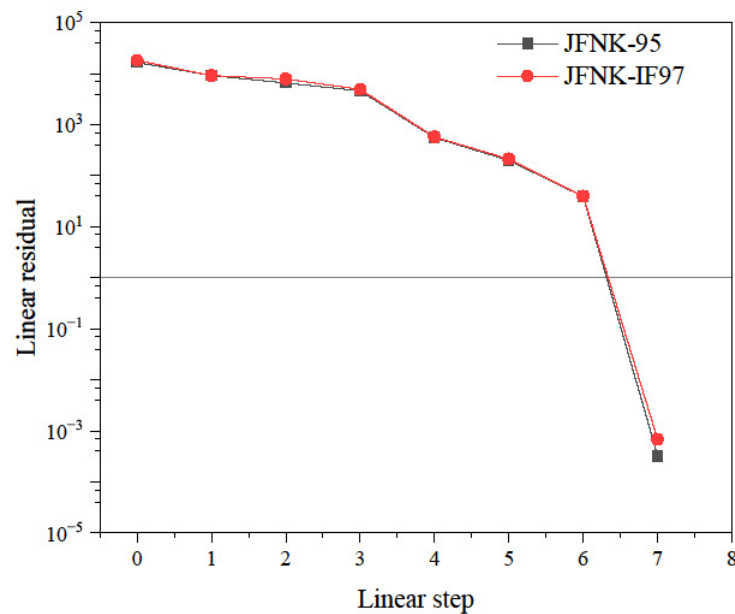


Figure 7. Linear residual history in steady-state HTR-10 steam generator simulation.

4.3. Transient H-OTSG Model in HTR-10

Illustrating the efficiency and reliability of the developed method is the main work of the paper. Three transient cases are investigated in the HTR-10 once-through steam generator. The time discretization used here is a first-order backward Euler scheme, which provides a fully implicit form with good accuracy and does not withstand much computational cost. The length of the time step is selected as $\Delta t = 0.5$ s. The simulation time of all the transients in this subsection is $t = 0 \sim 1000$ s, in order to facilitate the subsequent efficiency analysis. Through the analysis of the previous subsection, it can be concluded that the algorithms will only change the calculation efficiency and convergence characteristics without affecting the results. Therefore, the analysis here pays more attention to the influence of two water properties evaluation methods.

The first transient case is to change the inlet helium temperature of the HTR-10 steam generator by a 2% step increase. The water temperature at the outlet is selected as the key parameter because it reflects the overall steam generator calculation results and affects the simulations of the secondary circuit in the reactor system. The water temperature curve at the steam generator outlet is shown in Figure 8. The reference points in Figure 8 are data from the literature [36]. As the inlet helium temperature rises, the heat exchange between the primary and secondary circuits increases. Meanwhile, the outlet water temperature rises rapidly and finally stabilizes. Figure 8 indicates that both water properties evaluation routines can provide accurate results. Using backward equations will underestimate the outlet water temperature in this case. Compared with the precise water evaluation routine, the relative errors of the two methods are plotted in Figure 9, where the position with the most significant error is $t = 9.5$ s, and the maximum deviation temperature is $\Delta T_{max} = -1.34$ °C. This transient case causes a 31 °C increase in outlet water temperature, so the maximum relative deviation is still within 5% of the total variation.

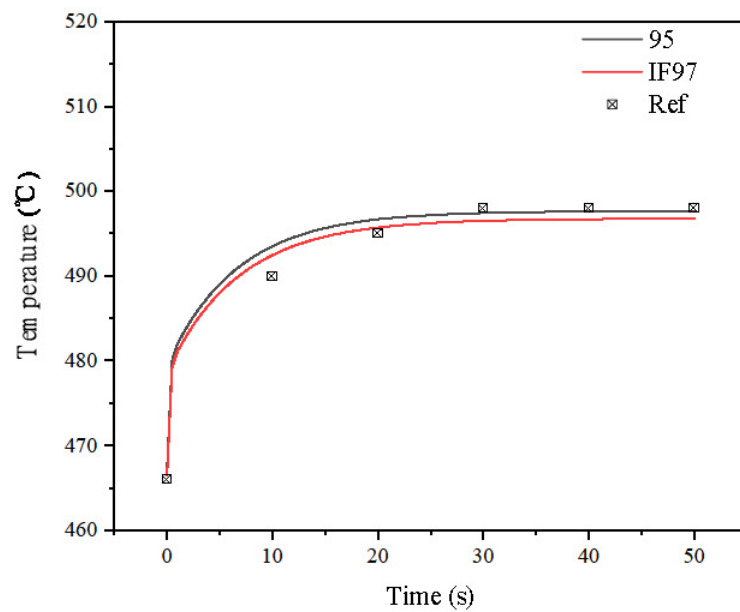


Figure 8. The outlet water temperature results of a 2% step increase in inlet helium temperature.

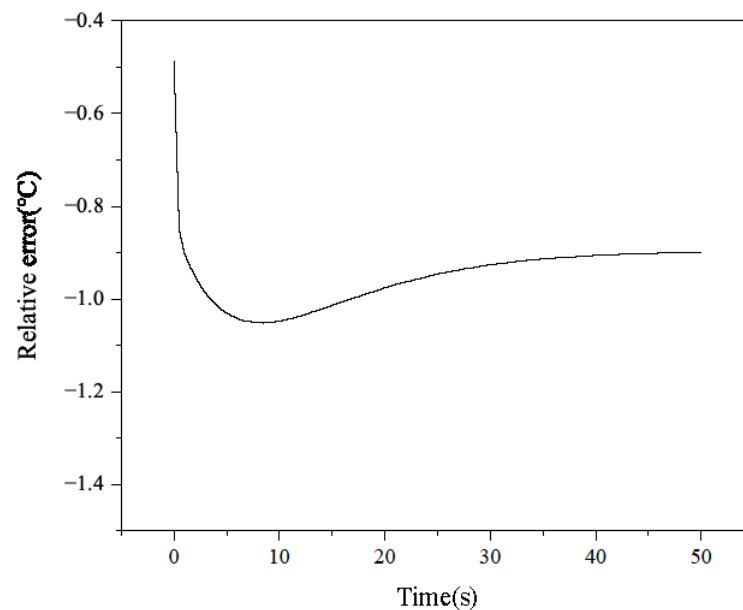


Figure 9. The relative error between the backward equation method and the original method of a 2% step increase in inlet helium temperature.

The second transient case changes the inlet water temperature of the HTR-10 steam generator by a 2% step increase. Different from the previous transient case, changing the temperature of the inlet water will not directly change the heat exchange, and the large heat capacity of water will lead to less temperature increase at the outlet than the previous case. At the beginning of the transient, there will be a temperature drop that meets the thermohydraulic mechanism. This is because the density decreases as the temperature of the inlet water increases, resulting in a decrease in overall steam generator pressure and an increase in mass flow in the superheated region. The effect of pressure changes is faster than temperature transfer, so the temperature of outlet water decreases at the beginning. According to the energy conservation, the outlet water will stabilize to a higher temperature. Both water properties evaluation routines can simulate this phenomenon and obtain good results in agreement with the reference solution, as shown in Figure 10.

The relative errors of the two methods are plotted in Figure 11, where relative deviation is stable at $\Delta T = 0.5\text{ }^{\circ}\text{C}$.

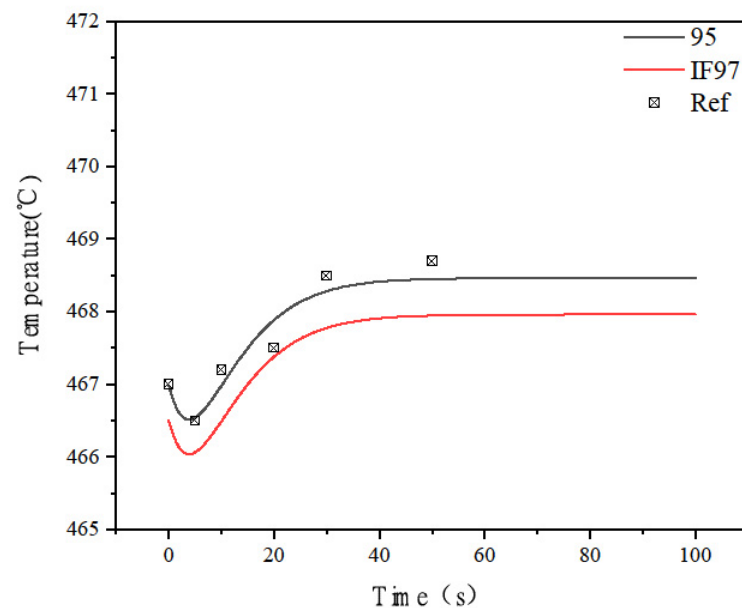


Figure 10. The outlet water temperature results of a 2% step increase in inlet water temperature.

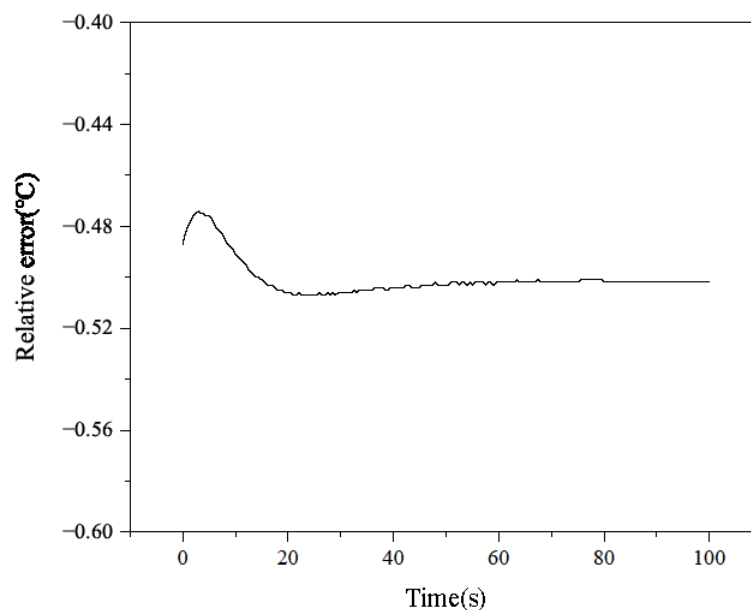


Figure 11. The relative error between the backward equation method and the original method of a 2% step increase in inlet water temperature.

The last transient case changes the inlet water pressure of the HTR-10 steam generator by a 5% step increase. Because the inlet pressure is changed directly, the procedure of the temperature change will be faster. The water temperature curve at the steam generator outlet is shown in Figure 12. The instantaneous change of inlet pressure will reduce the mass flow at the outlet, so that the steam temperature will rise at the beginning. The pressure variation decays, and, ultimately, the pressure of the outlet water will be higher than the initial value, resulting in a decrease in the steam temperature. Both water properties evaluation routines show good calculation results, and the relative deviation curve is drawn in Figure 13. Using the backward equations, the water property evaluation routine introduces deviations during the rapid transmission of pressure waves. The maximum

deviation temperature is $\Delta T_{max} = 1.03 \text{ }^\circ\text{C}$, which is about 8% deviation from the whole temperature fluctuation.

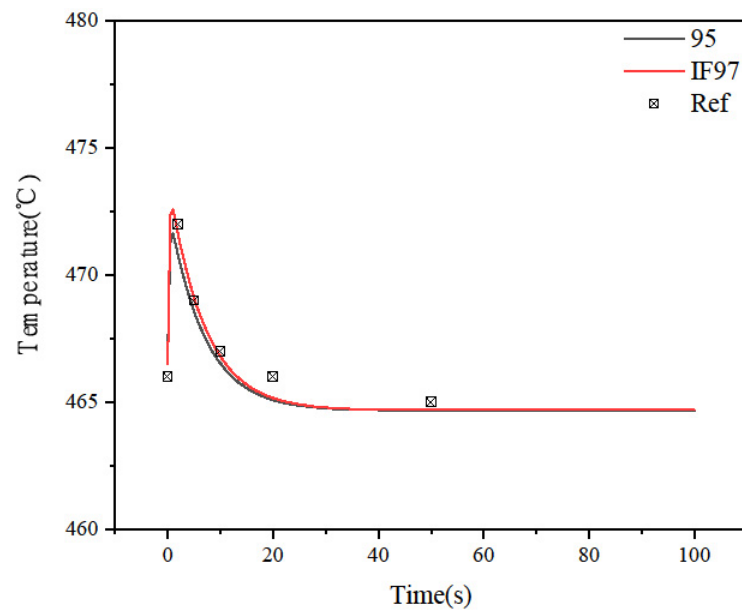


Figure 12. The outlet water temperature result of a 5% step increase in inlet water pressure.

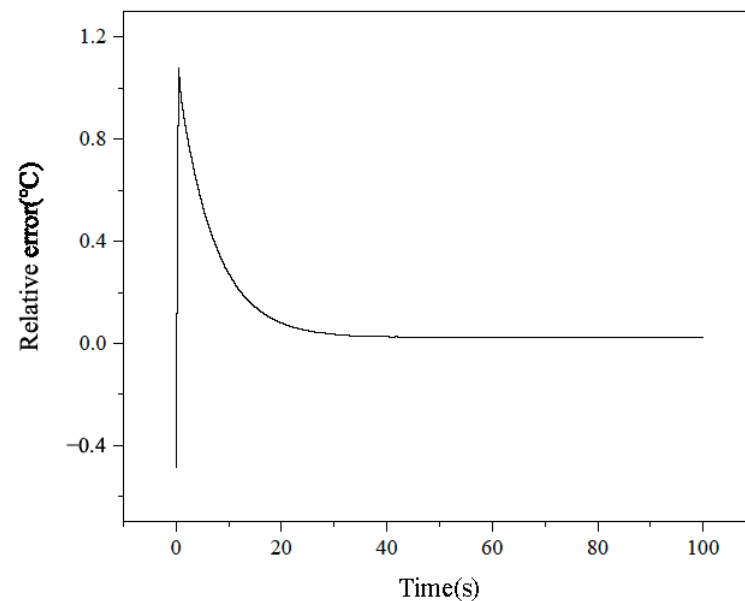


Figure 13. The relative error between the backward equation method and the original method of a 5% step increase in inlet water pressure.

The total simulation time with different algorithms and water properties evaluation routines in these three transients are summarized in Tables 9–11. The numbers of nonlinear and linear iterations are also listed. As shown, the JFNK method using backward equations to calculate water properties has the shortest calculation time. Although the JFNK method has the fastest computational efficiency, the computation cost fluctuates greatly under different transient conditions. This is due to the truncation error of the vector product using finite difference approximation without explicitly constructing the Jacobian matrix and results in the instability of the convergence property. The calculation time of the original algorithm will be reduced to 30% by using the backward equations for the water

properties calculation, which shows the same acceleration effect compared to the steady-state condition.

Table 9. Simulation time between different methods of step increase in inlet helium temperature.

	JFNK-95	JFNK-IF97	NK-95	NK-IF97
Total computational time (s)	1909.27	572.651	6517.1	2257.74
Numbers of nonlinear iterations	2614	2463	2888	2901
Numbers of linear iterations	64,214	61,171	24,354	20,472

Table 10. Simulation time between different methods of step increase in inlet water temperature.

	JFNK-95	JFNK-IF97	NK-95	NK-IF97
Total computational time (s)	1586.75	506.628	6498.31	2226.95
Numbers of nonlinear iterations	2082	2051	2867	2876
Numbers of linear iterations	55,803	54,740	24,927	20,389

Table 11. Simulation time between different methods of step increase in inlet water pressure.

	JFNK-95	JFNK-IF97	NK-95	NK-IF97
Total computational time (s)	2357.24	608.402	6520.84	2216.65
Numbers of nonlinear iterations	2856	2778	2894	2934
Numbers of linear iterations	68,187	65,099	24,372	20,564

5. Conclusions

The complex water and steam thermodynamic properties restrict the applications of H-OTSG simulation. Especially for HTGR, the higher primary inlet temperature will require a more accurate and stable H-OTSG simulation code. After analyzing the calculation cost of steam generator simulation, this work mainly focuses on the optimization of water and steam property evaluation and overall algorithm. A water property library is developed in the steam generator code based on the efficient formulation IAPWS-IF97. The results also prove that the code shows good performance during simulation. In order to meet the demand for fast simulation, simultaneous solution methods will also be used in the steam generator code to improve the convergence rate. Therefore, the Newton–Krylov and JFNK methods are implemented during steady-state and dynamic simulations. In order to verify the accuracy and efficiency of the code, three HTR-10 transients were studied and the results show that our code can accurately capture the dynamic behavior in the steam generator. The main results are as follows:

1. The developed water library exhibits good accuracy and consistency compared to the scientific formulation under the simulated operating conditions of the steam generator. The maximum relative error of thermodynamic properties is 1.7%, which proves the reliability of the water library. During H-OTSG simulation, the deviation of the main parameters between these two formulations is acceptable.
2. With the IAPWS-IF97 formulation, the calculation time of steady H-OTSG can be reduced by more than 60%. This illustrates the efficiency of this water property evaluation method, which is very useful for high-speed steam generator simulation.
3. A simultaneous solution algorithm also improves simulation performance greatly. In the steady-state simulation, the JFNK method can save about 80% calculation time compared with the Newton–Krylov method, since the Jacobian matrix is not explicitly constructed, while in different H-OTSG transients, the JFNK method can still same half calculation time.

Due to the use of many new techniques in H-OTSG simulation, our current work is still very preliminary, mainly to prove the efficiency and reliability of the method. More transient response cases of steam generators will be carried out in the future. Meanwhile, the applicability of the method to other steam generator models is also worth further study. The steam generator simulation analysis of the fixed-grid method is also in our future research plan.

Author Contributions: Conceptualization, Z.J.; Methodology, Y.W. and Z.J.; Validation, L.L. and H.T.; Investigation, Y.W.; Writing—original draft, Y.W. and Z.J.; Writing—review & editing, H.Z., J.G. and F.L.; Funding acquisition, H.Z. All authors have read and agreed to the published version of the manuscript.

Funding: This study is supported by National Natural Science Foundation of China No. 12275150, The National Key Research and Development Program of China No. 2022YFB1903000, and Beijing Natural Science Foundation No. 1212012.

Data Availability Statement: The data that support the findings of this study are available on request from the corresponding author, H.Z. upon reasonable request.

Conflicts of Interest: The authors declare no conflict of interest.

References

1. Wu, X.; Lin, D.; Zhong, D. The design features of the HTR-10. *Nucl. Eng. Des.* **2002**, *218*, 25–32. [[CrossRef](#)]
2. Hoffer, N.V.; Sabharwall, P.; Anderson, N.A. *Modeling a Helical-coil Steam Generator in RELAP5-3D for the Next Generation Nuclear Plant*; Idaho National Laboratory: Idaho Falls, ID, USA, 2011.
3. Esch, M.; Knoche, D.; Hurtado, A. Numerical discretization analysis of a HTR steam generator model for the thermal-hydraulics code trace. *Nucl. Technol. Radiat. Protect.* **2014**, *29*, 31–38. [[CrossRef](#)]
4. Caramello, M.; Bertani, C.; De Salve, M.; Panella, B. Helical coil thermal hydraulic model. *J. Phys. Conf. Ser.* **2014**, *547*, 12034. [[CrossRef](#)]
5. Yoon, J.; Kim, J.-P.; Kim, H.-Y.; Lee, D.J.; Chang, M.H. Development of a computer code, ONCESG, for the thermal-hydraulic design of a once-through steam generator. *J. Nucl. Sci. Technol.* **2012**, *37*, 445–454. [[CrossRef](#)]
6. Xia, G.; Yuan, Y.; Peng, M.; Lv, X.; Sun, L. Numerical studies of a helical coil once-through steam generator. *Ann. Nucl. Energy* **2017**, *109*, 52–60. [[CrossRef](#)]
7. Li, W.C.; Wang, J.J.; Sun, Z.N.; Liu, J.; Meng, Z. Experimental investigation on thermal stratification induced by steam-air mixture vertical injection with shallow submergence depth. *Prog. Nucl. Energy* **2019**, *115*, 52–61. [[CrossRef](#)]
8. Wu, Y.; Liu, B.; Zhang, H.; Zhu, K.; Kong, B.; Guo, J.; Li, F. Accuracy and efficient solution of helical coiled once-through steam generator model using JFNK method. *Ann. Nucl. Energy* **2021**, *159*, 108290. [[CrossRef](#)]
9. Wagner, W.; PruB, A. The IAPWS Formulation 1995 for the Thermodynamic Properties of Ordinary Water Substance for General and Scientific Use. *J. Phys. Chem. Ref. Data* **2002**, *31*, 387–535. [[CrossRef](#)]
10. Keenan, J.H.; Keyes, F.G.; Hill, P.G.; Moore, J.G. *Steam Tables*; Wiley Interscience: New York, NY, USA, 1969.
11. Sail, A.; Wagner, W. A fundamental equation for water covering the range from melting ice to 1273K at pressure up to 25,000 Mpa. *J. Phys. Chem. Ref. Data* **1989**, *18*, 1537–1564. [[CrossRef](#)]
12. Fernandes, J.L. Fast evaluation of thermodynamic properties of superheated steam: A cubic equation of state. *Appl. Therm. Eng.* **1996**, *16*, 71–79. [[CrossRef](#)]
13. International Association for the Properties of Water and Steam. *IAPWS Industrial Formulation 1997 for the Thermodynamic Properties of Water and Steam*; IAPWS Release, IAPWS Secretariat: Oklahoma City, OK, USA, 1997.
14. Esmaili, H.; Kazeminejad, H.; Khalafi, H.; Mirvakili, S. Subchannel analysis of annular fuel assembly using the preconditioned Jacobian-free Newton Krylov methods. *Ann. Nucl. Energy* **2020**, *146*, 107616. [[CrossRef](#)]
15. He, Q.; Zhang, Y.; Liu, Z.; Cao, L.; Wu, H. The JFNK method for the PWR's transient simulation considering neutronics, thermal hydraulics and mechanics. *Nucl. Eng. Technol.* **2020**, *52*, 258–270. [[CrossRef](#)]
16. Liu, B.; Wu, Y.; Guo, J. Finite difference Jacobian based Newton-Krylov coupling method for solving multi-physics nonlinear system of nuclear reactor. *Ann. Nucl. Energy* **2020**, *148*, 107670. [[CrossRef](#)]
17. Balestra, P.; Schunert Carlsen, R.; Carlsen, R.W.; Novak, A.J.; DeHart, M.D.; Martineau, R.C. PBMR-400 Benchmark solution of exercise 1 and 2 using the moose based application: Mammoth, Pronghorn. *Eur. Phys. J. Conf.* **2021**, *247*, 6020. [[CrossRef](#)]
18. Wu, Y.; Liu, B.; Zhang, H.; Guo, J.; Li, F. A Movable Boundary Model for Helical Coiled Once-Through Steam Generator using Preconditioned JFNK method. *Int. J. Adv. Nucl. React. Des. Technol.* **2022**, *4*, 1–8. [[CrossRef](#)]
19. Liu, L.; Wu, Y.; Liu, B.; Zhang, H.; Guo, J.; Li, F. A modified JFNK method for solving the fundamental eigenmode in k-eigenvalue problem. *Ann. Nucl. Energy* **2021**, *167*, 108823. [[CrossRef](#)]
20. Gaston, D.; Permann, C.; Peterson, J.; Slaughter, A.E.; Andrš, D.; Wang, Y.; Short, M.P.; Perez, D.M.; Tonks, M.R.; Ortensi, J.; et al. Physics-based multiscale coupling for full core nuclear reactor simulation. *Ann. Nucl. Energy* **2015**, *84*, 45–54. [[CrossRef](#)]

21. Zhang, H.; Guo, J.; Lu, J.; Li, F.; Xu, Y.; Downar, T.J. An assessment of coupling algorithms in HTR simulator TINTE. *Nucl. Sci. Eng.* **2018**, *190*, 287–309. [[CrossRef](#)]
22. Knoll, D. Jacobian-free Newton-Krylov methods: A survey of approaches and applications. *J. Comput. Phys.* **2004**, *193*, 357–397. [[CrossRef](#)]
23. Wagner, W.; Cooper, J. The IAPWS industrial formulation 1997 for the thermodynamic properties of water and steam. *J. Eng. Gas Turbines Power* **2000**, *122*, 150–182. [[CrossRef](#)]
24. International Formulation Committee of the 6th International Conference on the Properties of Steam. *The 1967 IFC Formulation for Industrial Use*; Verein Deutscher Ingenieure: Düsseldorf, Germany, 1967.
25. Gedde, U.W. *Essential Classical Thermodynamics*; Springer Nature: Berlin/Heidelberg, Germany, 2020.
26. Kretzschmar, H.J.; Wagner, W. *International Steam Tables: Properties of Water and Steam Based on the Industrial Formulation IAPWS-IF97*; Springer Science & Business Media: Berlin/Heidelberg, Germany, 2007.
27. Setzmann, U.; Wagner, W. A New Method for Optimizing the Structure of Thermodynamic Correlation Equations. *Int. J. Thermophys.* **1989**, *10*, 1103–1126. [[CrossRef](#)]
28. The International Association for the Properties of Water and Steam. *Release on the IAPWS Formulation 2008 for the Viscosity of Ordinary Water Substance*; IAPWS: Berlin, Germany, 2008.
29. The International Association for the Properties of Water and Steam. *Release on the IAPWS Formulation 2011 for the Thermal Conductivity of Ordinary Water Substance*; IAPWS: Plzeň, Czech Republic, 2011.
30. Li, H.; Huang, X.; Zhang, L. A lumped parameter dynamic model of the helical coiled once-through steam generator with movable boundaries. *Nucl. Eng. Des.* **2008**, *238*, 1657–1663. [[CrossRef](#)]
31. Zhu, J.; Guo, Y.; Zhang, Z. Dynamic simulation of once-through steam generator with concentric annuli tube. *Ann. Nucl. Energy* **2020**, *50*, 185–198. [[CrossRef](#)]
32. Wolfe, P. Convergence conditions for ascent methods. ii: Some corrections. *Siam Rev.* **1971**, *13*, 185–188. [[CrossRef](#)]
33. Bi, Q.; Chen, T.; Luo, Y. Frictional pressure drop of steam-water two phase flow in helical coils with small helix diameter of htr-10. *Chin. J. Nucl. Sci. Eng.* **1991**, *16*, 208–213.
34. Balay, S.; Abhyankar, S.; Adams, M.; Benson, S.; Brown, J.; Brune, P.; Buschelman, K.; Constantinescu, E.; Dalcin, L.; Dener, A.; et al. *PETSc User's Manual. Technical Report ANL-21/39—Revision 3.18*; Argonne National Laboratory: Lemont, IL, USA, 2018.
35. Bell, H.; Wronski, J.; Quoilin, S.; Lemort, V. Pure and Pseudo-pure Fluid Thermophysical Property Evaluation and the Open-Source Thermophysical Property Library CoolProp. *Ind. Eng. Chem. Res.* **2014**, *53*, 2498–2508. [[CrossRef](#)] [[PubMed](#)]
36. Huang, X. *Dynamic Models of 10MW High Temperature Gas-Cooled Reactor and Studies on Its Dynamic Character*. Ph.D. Thesis, Tsinghua University, Beijing, China, 1998.

Disclaimer/Publisher's Note: The statements, opinions and data contained in all publications are solely those of the individual author(s) and contributor(s) and not of MDPI and/or the editor(s). MDPI and/or the editor(s) disclaim responsibility for any injury to people or property resulting from any ideas, methods, instructions or products referred to in the content.